

On the a and g Families of Symmetric Periodic Orbits in the Photo-Gravitational Hill Problem and Their Application to Asteroids*

D. García Yárnoz[†], D. J. Scheeres[‡] and C. R. McInnes[§]

This paper focuses on the exploration of families of planar symmetric periodic orbits around minor bodies under the effect of solar radiation pressure. For very small asteroids and comets, an extension of the Hill problem with Solar Radiation Pressure (SRP) perturbation is a particularly well-suited dynamical model. The evolution of the a and g families of symmetric periodic orbits has been studied in this model when SRP is increased from the classical problem with no SRP to levels corresponding to current and future planned missions to minor bodies, as well as one extreme case with very large SRP. In addition, the feasibility and applicability of these orbits for the case of asteroids was analysed, and the effect of SRP in their stability is presented.

I. Introduction

THE influence of solar radiation pressure perturbation on spacecraft dynamics is of great importance for asteroid exploration missions. In the course of a previous study,¹ the authors encountered a series of periodic solutions propagated with a numerical integrator considering the gravitational attraction of a small asteroid and the Sun, and including SRP and eclipses (see Figure 1). These orbits are symmetric with respect to the x-axis in a synodic frame co-rotating with the asteroid around the Sun (and thus they have two crossings perpendicular to this axis). They have two or more inversions of the orbit direction, that take place when they reach the zero-velocity curves for their particular energy level, alternating between prograde and retrograde sections of the orbit from the point of view of the body. Of particular interest for operations around asteroids would be orbits with retrograde sections close to the asteroid, and prograde ones far from it (e.g. second plot in Figure 1), as retrograde orbits are less affected by the highly non-spherical gravity fields of minor bodies.

The first two classes of orbits were identified as members of the well-known a and g' families of symmetric periodic orbits of the Circular Restricted Three Body Problem (CR3BP), as described by Hénon.² In particular, the top branch of Hénon's g' family greatly resembles the type of orbits with one loop and two inversions that were found in the numerical propagation analysis. The following sections present the evolution of these families when solar radiation pressure is introduced and study the applicability of these orbits for minor bodies.

A. Families of symmetric periodic orbits in the CR3BP

In his 1969 paper, Hénon explored families of symmetric periodic orbits in the planar case of the CR3BP for a very small secondary (limiting case of Hill). Hénon concentrated on simple-periodic cases (orbits with only two crossings of the x-axis), although the aforementioned branch of the g' family has 4 crossings and is thus double-periodic according to Hénon's own definition. He systematically mapped the planar problem, and cross-checked the validity of previous symmetric periodic solutions reported by Hill himself, Lord Kelvin, Jackson and the outputs of the more thorough search by Matukuma;³⁻⁵ and studied the in-plane stability of these solutions.

This series of families in the CR3BP have been extensively studied and are still of great interest. Besides the references used by Hénon in his classical series of papers, other authors came across orbits of the a , g and g' family, albeit for different mass ratios (no longer Hill problem). Darwin⁶ presented an incomplete map of various classes of orbits for a mass ratio of 1/11 (he studies a fictitious Sun-Jupiter case with a much larger mass for Jupiter), which

* An updated version of this paper has been submitted for publication to *Celestial Mechanics and Dynamical Astronomy*

[†] Advanced Space Concepts Laboratory, Dept. of Mechanical and Aerospace Engineering, University of Strathclyde, Glasgow G1 1XQ, UK. E-mail: daniel.garcia-yarnoz@strath.ac.uk Telephone: +44 (0)141 444 8316. Fax: +44 (0)141 552 5105

[‡] Celestial and Spaceflight Mechanics Laboratory, University of Colorado at Boulder.

[§] Advanced Space Concepts Laboratory, Dept. of Mechanical and Aerospace Engineering, University of Strathclyde

corresponds to a section of the g - g' family. Broucke⁷ presented the results previously obtained in his thesis for orbit families in the Earth-Moon system. Szebehely worked on these same sets of periodic orbits.⁸ His book *Theory of Orbits*⁹ is still a classic reference with an extensive study on different families in the CR3BP, mostly for equal masses (the so-called Copenhagen problem), but also reviewing and completing Darwin's and Broucke's work. Hénon had also studied prior to Hill problem planar symmetric families in the Copenhagen problem as the other limiting case of the CR3BP.¹⁰ In fact, the naming convention assigning letters for the orbit families followed by Szebehely and Hénon actually spawns from the nomenclature Strömgren introduced for families of solutions for the Copenhagen problem decades before.¹¹ Family a is also sometimes referred to in literature as planar Lyapunov orbits, while certain sections of family g are also referred to as Distant Prograde Orbits (DPO).

Hénon continued studying the vertical stability of these families in the equal masses case¹² and the Hill problem.¹³ Michalodimitrakis¹⁴ later extended the work of Hénon by studying some 3-dimensional families of orbits branching off from the vertical critical orbits in the planar case. Perko¹⁵ established the existence of the families a , c , f , g , g' , g'' ... mapped by Hénon² for the case of small $\mu > 0$. He overlaps his families over Hénon's, showing their similarity. An additional paper of Hénon,¹⁶ in which he came back to the same problem after over 30 years, expanded his search to double and triple-periodic orbits as well. He follows the stricter definition of N -periodic or multiplicity N : orbits with $2N$ crossings of the x -axis. With this definition the type of trajectories presented in Figure 1 are simple-periodic, double periodic, 5-periodic, and 8-periodic (2, 4, 10 and 16 crossings of the x -axis respectively). A few years later, Hénon¹⁷ revisited once more the Hill problem to study asymmetric periodic solutions.

Finally, Lara and Russell¹⁸ performed a comprehensive review of the g family for different mass ratios (explaining and comparing among others Darwin's results for the fictitious Sun-Jupiter case⁶ or Broucke's for the Earth-Moon system⁷), including applications for a Jupiter-Europa orbiter.¹⁹ Two recently published papers by Batkhin,^{20, 21} presented an algorithm with regularized coordinates to systematically obtain all families reported by Hénon for Hill problem plus a set of additional families including multiple collisions with the secondary body. On private conversation with Patricia Verrier²² to discuss the branching and connections between two-dimensional and three-dimensional families, she reported that she was studying families of period-doubling bifurcations from halo orbits for the Earth-Moon mass ratio (which she names U1 and U2), that resemble planar g' orbits. She reports a connection with the g' family and has proved the existence of this connection also in the Hill problem.

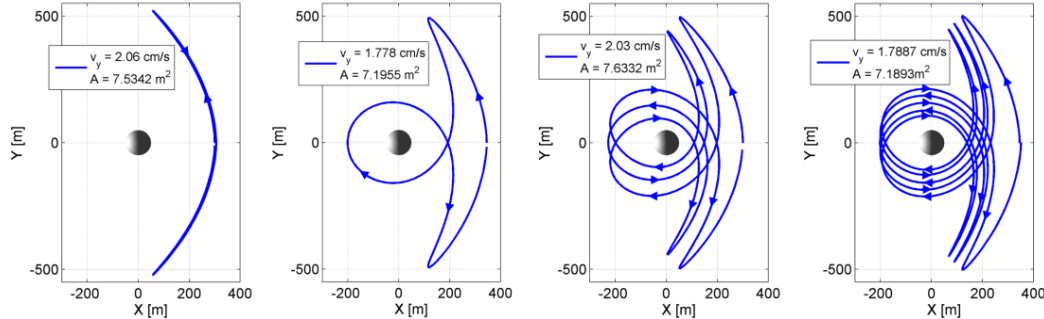


Figure 1. Families of solutions in a co-rotating synodic frame.

B. Extending Hill problem with SRP

Hill's limiting case of the CR3BP is particularly suited to the study of spacecraft trajectories in the vicinity of asteroids, as the mass of the asteroid can be considered negligible with respect to the Sun, leading to very low mass ratios. However, SRP plays an important role around these minor bodies. It is arguably the largest perturbing force for spacecraft with typical area to mass ratios. Its effect on the well-known symmetric periodic orbit solutions of the CR3BP has not been studied in such great detail.

Approaching the classical photo-gravitational CR3BP,^{23, 24} Papadakis²⁵ studied the evolution of planar symmetric families in the equal masses case (Copenhagen problem) with two radiating bodies. This approximation has interesting applications in the study of accretion disks around binary stars. Markellos et al.²⁶ studied the limiting case of Hill for different configurations of the radiating bodies, and later analyzed the evolution of families of periodic orbits up to high multiplicity (16-periodic) and their stability.²⁷ A more comprehensive analysis using regularized coordinates covering symmetric periodic orbits up to multiplicity 81 can be found in Ref. 28. These studies limit themselves though to low levels of solar radiation pressure, applicable to a star-planet case, but falling short for the case of asteroids.

II. The photo-gravitational Hill problem

For the analysis in this paper we part from the classical equations of motion for the CR3BP in the synodic frame centred in the barycentre of the system:

$$\ddot{\vec{r}} + 2\Omega(\hat{k} \times \dot{\vec{r}}) + \Omega^2 \hat{k} \times (\hat{k} \times \vec{r}) = -\mu \frac{(\vec{r} - \vec{r}_A)}{|\vec{r} - \vec{r}_A|^3} - (1-\mu)(1-\beta) \frac{(\vec{r} - \vec{r}_S)}{|\vec{r} - \vec{r}_S|^3} \quad (1)$$

where distances have already been normalized by the radius of the circular orbit of the asteroid d . The subscripts A and S represent the asteroid and the Sun respectively, and the Sun or more massive body is assumed on the left (contrary to the convention used in Szebehely⁹). The mass ratio μ and mean motion Ω are given by:

$$\begin{aligned} \mu &= \mu_A / (\mu_A + \mu_S) \\ \Omega &= \sqrt{(\mu_A + \mu_S) / d^3} \end{aligned} \quad (2)$$

The lightness number β in Eq. (1) represents the ratio of the solar radiation pressure and the gravitation of the Sun, defined as:

$$\beta = \frac{LQ}{4\pi c \mu_S} \frac{A}{m} \quad (3)$$

where L is the solar luminosity, Q the solar radiation pressure coefficient, which depends on the material properties, c is the speed of light, μ_S is again the gravitational constant of the Sun, and A/m is the area to mass ratio of the spacecraft. The solar radiation pressure force has been modelled with the so-called cannon-ball approach, assuming the spacecraft has a constant effective area always perpendicular to the Sun-spacecraft line, with the only component of the force in the radial direction.

Following Hénon,² we normalize the time with the inverse of the mean motion and apply a change of reference frame centre, time normalisation, and scaling of distances by $\mu^{1/3}$:

$$\begin{aligned} \vec{r}(t) &= (x, y, z, \dot{x}, \dot{y}, \dot{z})^T & x &= 1 - \mu + \mu^{1/3} \xi & \dot{x} &= \mu^{1/3} \Omega \xi' \\ & \downarrow & y &= \mu^{1/3} \eta & \dot{y} &= \mu^{1/3} \Omega \eta' \\ \vec{\rho}(\tau) &= (\xi, \eta, \zeta, \xi', \eta', \zeta')^T & z &= \mu^{1/3} \zeta & \dot{z} &= \mu^{1/3} \Omega \zeta' \\ & & t &= \tau / \Omega & (\dot{a} &= da/dt; a' = da/d\tau) \end{aligned} \quad (4)$$

The lightness number is also scaled with $\mu^{1/3}$ as the distances:

$$\beta_0 = \beta / \mu^{1/3} \quad (5)$$

Assuming the mass ratio μ small, and keeping only terms $\mu^{2/3}$ or larger, the classical Jacobi constant in the rotating frame, given by:

$$C = \Omega^2 (x^2 + y^2) + 2\mu_S (1-\beta) / r_S + 2\mu_A / r_A - \dot{x}^2 - \dot{y}^2 - \dot{z}^2 \quad (6)$$

then becomes:

$$C = 3 - 2\mu^{1/3} \beta_0 + \mu^{2/3} (3\xi^2 - \zeta^2 + 2\beta_0 \xi + 2/\sqrt{\xi^2 + \eta^2 + \zeta^2} - \xi'^2 - \eta'^2 - \zeta'^2) \quad (7)$$

As the first part is constant (for a given lightness number and mass ratio), similarly to Hénon we can define a new Jacobi constant Γ given by:

$$\Gamma = (C - 3 + 2\mu^{1/3} \beta_0) / \mu^{2/3} = 3\xi^2 - \zeta^2 + 2\beta_0 \xi + 2/\sqrt{\xi^2 + \eta^2 + \zeta^2} - \xi'^2 - \eta'^2 - \zeta'^2 \quad (8)$$

Finally, the equations of motion in the rotating frame $\vec{\rho}' = \vec{F}(\vec{\rho})$ take the well known form:

$$\begin{cases} \xi'' = 2\eta' + 3\xi - \xi / (\xi^2 + \eta^2 + \zeta^2)^{3/2} + \beta_0 \\ \eta'' = -2\xi' - \eta / (\xi^2 + \eta^2 + \zeta^2)^{3/2} \\ \zeta'' = -\zeta - \zeta / (\xi^2 + \eta^2 + \zeta^2)^{3/2} \end{cases} \quad (9)$$

These are equivalent to the EOM defined in Byram and Scheeres²⁹ or Broschart et al.³⁰

A. The a , g and g' families in the original Hill problem

The former equations reduce to the set studied by Hénon² when equating the lightness number to zero. This set of equations does not depend then on any additional parameter. The same planar periodic families of orbits symmetric with respect to the ξ -axis were reproduced using Hénon's reported values as initial guesses.

We concentrate in this paper on the families in the vicinity of the L_2 region. With the introduction of SRP, this region is reduced in size and is closer to the secondary, while the L_1 point migrates far in the direction of the radiating primary and its associated families of orbits are thus of less interest for the observation of an asteroid. Only simple-periodic families (and a double-periodic branch) were considered as in the original paper by Hénon. Figure 2 represents the solution map around L_2 in the $\Gamma - \xi$ space, with ξ representing the initial position along the ξ -axis.

The initial conditions were selected as a perpendicular crossing point of the ξ -axis with positive η' . The shaded patch represents the forbidden region, given by:

$$\Gamma > 3\xi^2 + 2\beta_0\xi + 2/\xi \quad (10)$$

It can be observed that family a , or the planar Lyapunov family (Figure 3 top left) originates from L_2 (black x marker) and terminates asymptotically at $\xi = 0$.

Family g (Figure 3 top right) starts off at a negative Jacobi constant as large ribbon-type orbits with crossings very close to the secondary body. As the Jacobi constant increases, the ribbon shape disappears and they become circular. There is a bifurcation point (black dot marker) from where another planar subfamily originates (labelled g'). The branch of the g family to the right of the bifurcation point consists of decreasingly smaller almost circular orbits around the secondary.

Family g' bifurcates from an almost circular orbit of the g family. The branch to the top of the bifurcation point has a collision point (black + marker) with the secondary. To the left of the collision point family g' is double periodic (4 intersections with the x-axis, Figure 3 bottom left) and follows closely the a family in the $\Gamma - \xi$ space. To the right of the collision point (Figure 3 bottom right) and above the bifurcation, family g' consists for the most part of a series of oval-shaped orbits extending towards the right. Below the circular orbit at the bifurcation point the oval orbits continue extending towards the left until their shape starts deforming with ribbon-like loops again. There is another collision point (not indicated) with the secondary at $\xi = 0$ and the g' family continues in the negative ξ quadrant after the collision. This part of the family has not been studied in this paper.

Orbits intersecting the secondary body surface for an average asteroid density of 2.6 g/cm^3 are plotted with a dashed line. It is not surprising that this region is around the collision point.

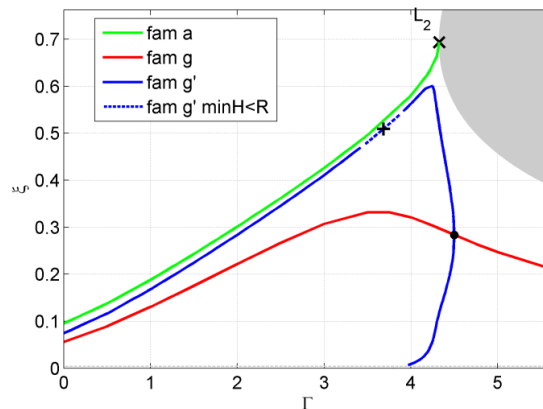


Figure 2: Solution map of the symmetric periodic families around L_2 in the CR3BP

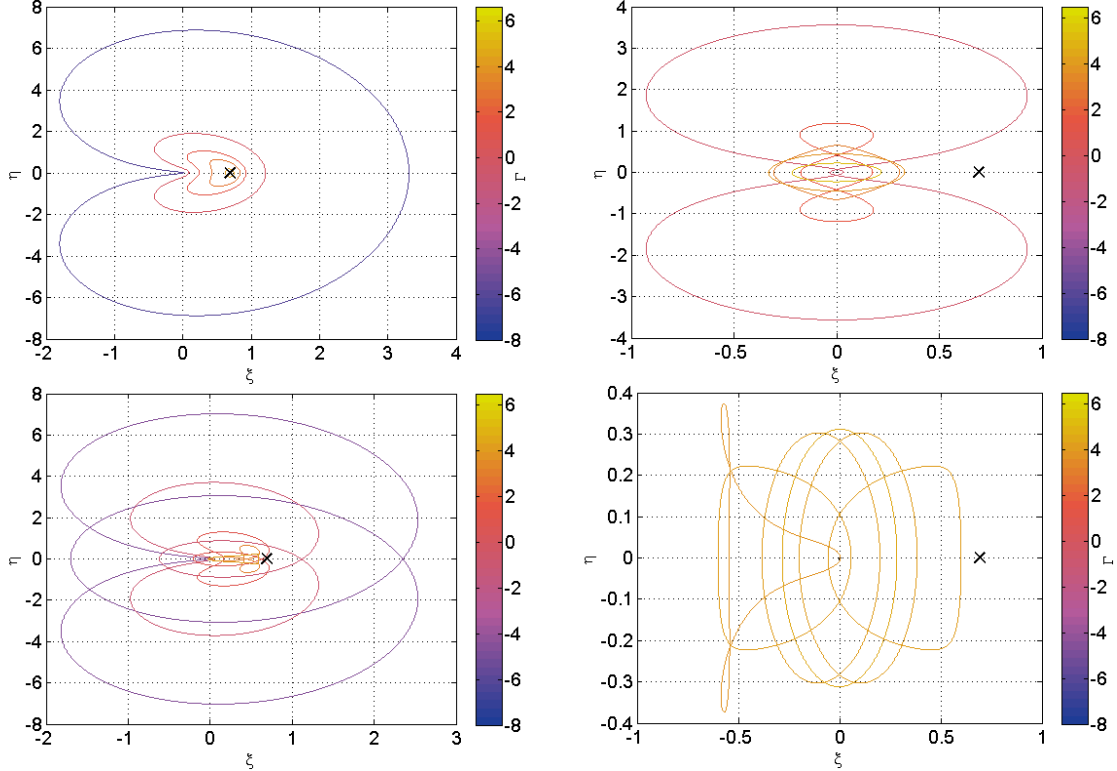


Figure 3: Families a (top left), g (top right) and g' (bottom, split in two branches) in the Hill problem with no solar radiation pressure

B. Evolution with lightness number

By means of a continuation method, we increase the value of β_0 up to more realistic lightness numbers. For currently flying and planned minor body orbiters the lightness number is usually of the order of 20-30.³¹ We also consider an extreme case with a β_0 value of approximately 684 (corresponding to a small 50 m radius asteroid at 1 AU, average asteroid density of 2.6 g/cm³, 100 kg spacecraft mass and 8 m² effective area).

Figure 4 shows the evolution of the families with increasing β_0 . The L_2 point position on the ξ -axis decreases, while its Jacobi constant increases with lightness number. The bifurcation point of the g - g' families disappears immediately for small lightness numbers resulting in two unconnected families (in the plane, there could still be connections through intermediate three-dimensional families). Arbitrarily, the g family was assumed now to contain the branch of the original g family left of the bifurcation point, and the branch of the original g' family to the bottom of the bifurcation point (see Figure 4). The g' family now contains the top branch of the original g' , which includes the collision point and the double-periodic section, and the right branch of the original g family including decreasingly smaller orbits around the secondary.

The new g family reduces its size and the maximum ξ crossing decreases rapidly. It then disappears for large lightness numbers. The right branch of the new g' family on the other hand quickly tends to skirt the border of the forbidden region, tending to linear degenerate orbits along the ξ -axis. Meanwhile, the collision point that separates the simple and double periodic portions of the new g' family migrates towards the L_2 point.

This behaviour is similar to the one observed in the study of radiating equal masses,²⁵ and continues the results obtained in Kanavos et al.²⁷ for lightness numbers up to 0.33. The following sections show the changes in the shape of the orbits with SRP.

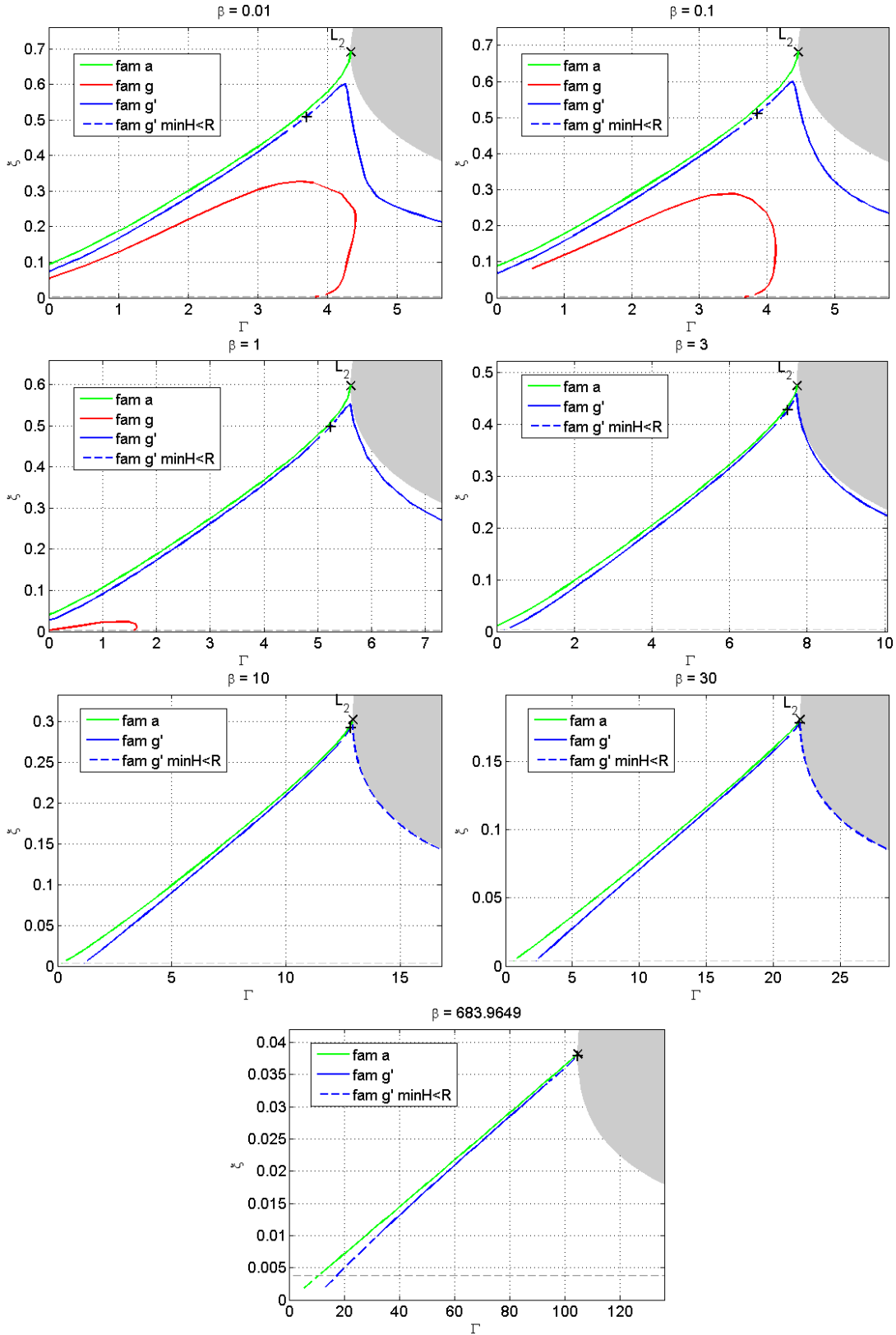


Figure 4: Solution map evolution with increasing lightness number β_0

1. Family *a*

Figure 5 shows the evolution of the *a* family from bean-shaped to boomerang-like orbits.

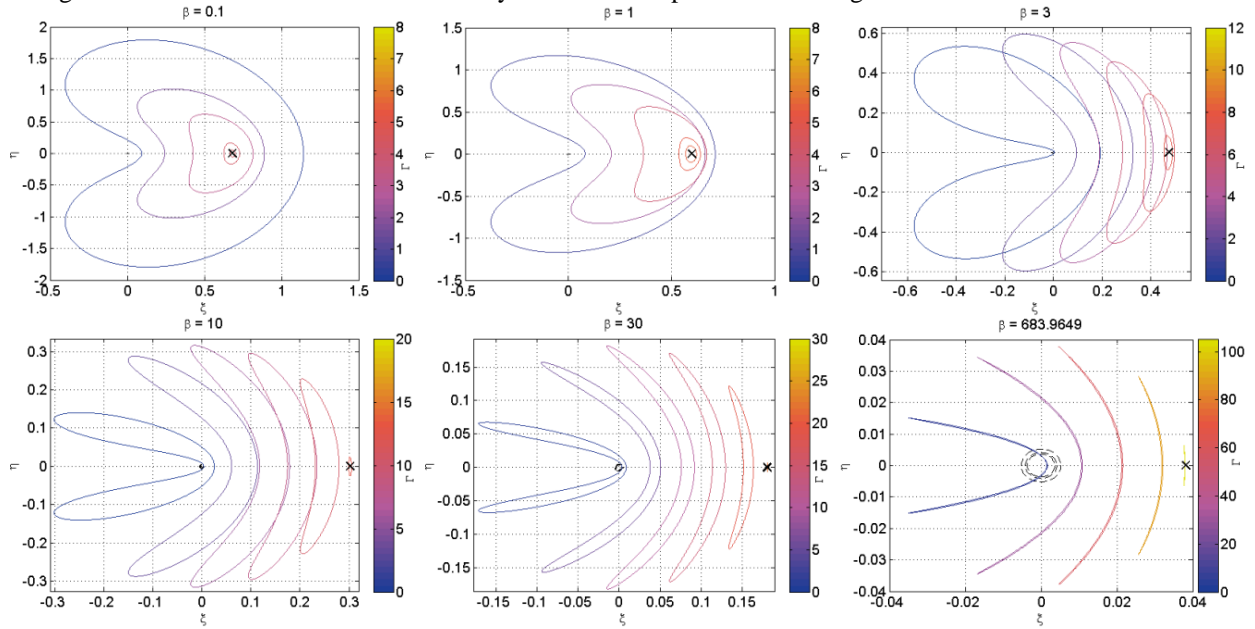


Figure 5: Family *a* evolution with increasing lightness number

2. Family *g-g'*

Figure 6 plots orbits of the left branch of the *g'* family up to the maximum value of ξ crossing for various Jacobi constants. This includes the double periodic branch left of the collision point plus a few oval-shaped simple periodic orbits.

Figure 7 plots orbits of the right branch of the *g'* family from the maximum value of ξ crossing for various Jacobi constants. In the case of no SRP (see Figure 3), family *g'* continued with oval-shaped orbits oriented towards the left until the collision point at $\xi = 0$. In Figure 7, the branch now includes the former part of the *g* family which consisted of direct orbits around the secondary of reducing size.

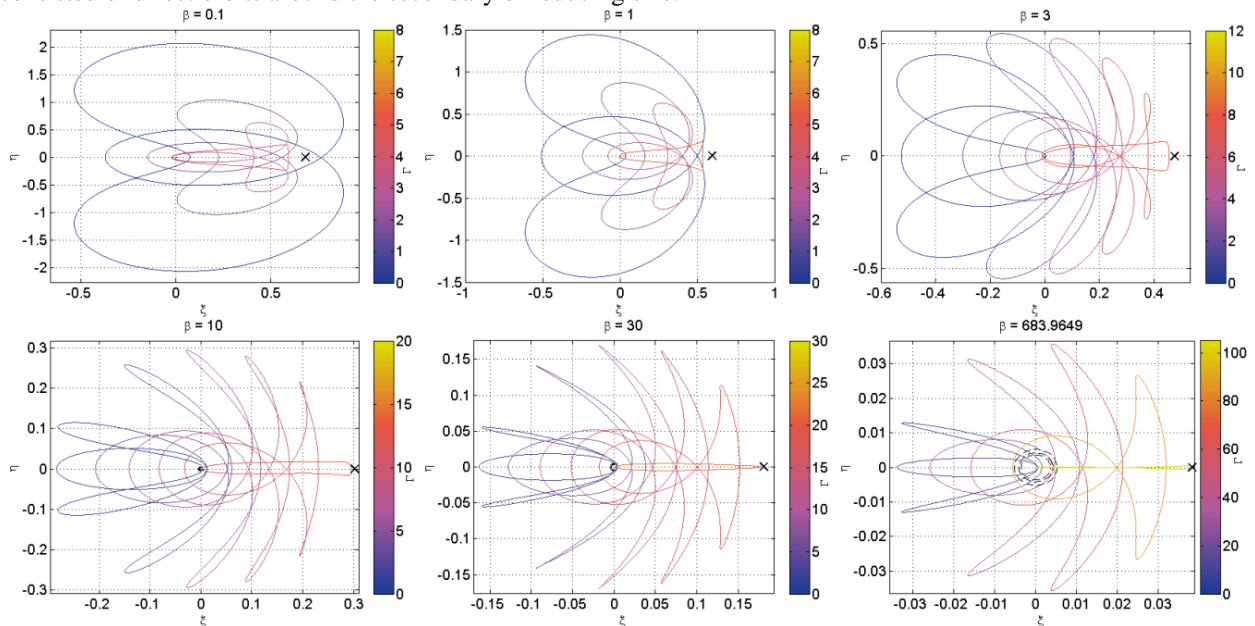


Figure 6: Family *g'* (left branch) evolution with increasing lightness number

Figure 8 plots orbits of the g family from the maximum value of ξ crossing for various Jacobi constants. Family g transitions from the ribbon-type orbits in the original g family to the left-extending oval-shape orbits in the original g' . For a lightness number of 1 the orbits transition between the two ribbon-type orbits without an oval-shape phase.

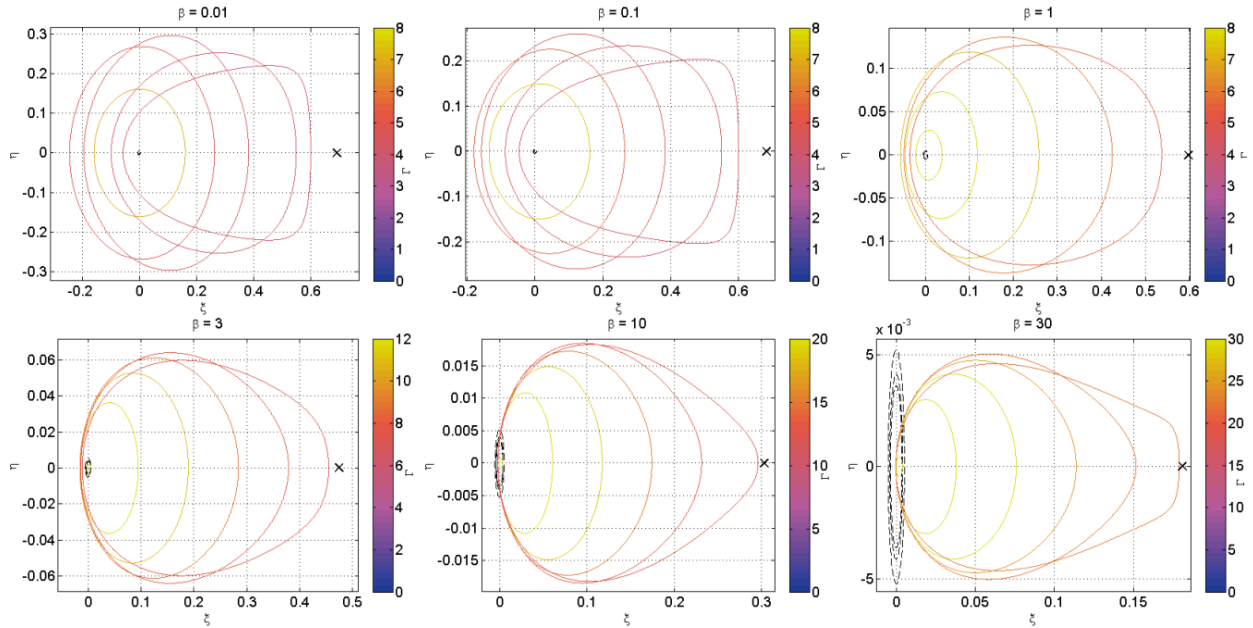


Figure 7: Family g' (right branch) evolution with increasing lightness number

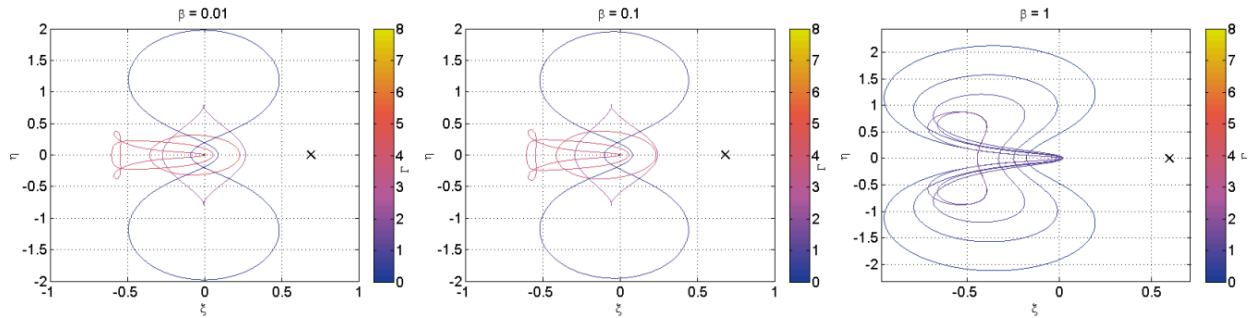


Figure 8: Family g evolution with increasing lightness number

C. Feasibility of the single periodic g' family solutions

The right section of the new g' family appears to always intersect the asteroid surface for high lightness numbers (dashed lines in Figure 4 represent intersection with the secondary). To better estimate if there is a size of asteroids for which these orbits do not intersect the surface, the radius of the surface has been plotted in the normalised and scaled space ξ and η' . The asteroid radius (assumed a spherical body) in scaled coordinates is fixed for a given density, and can be calculated as:

$$R_{norm} = \frac{1}{d} \sqrt[3]{\frac{3\mu_s}{4\pi\rho G}} \quad (11)$$

This allows us to plot with dashed black lines in Figures 5 to 7 three circles representing the asteroid surface for densities of 1, 2 and 3 g/cm^3 respectively, assuming a distance d to the asteroid of 1 AU. These lines indicate that for realistic densities the right branch of the g' family intersects the surface for large β_0 . It is particularly noticeable for the bottom right plot of Figure 7.

In Figure 9 the maximum pericentre height for the right branch of the new g' family and the maximum ξ crossing of the g family have been plotted as a function of the lightness number. Horizontal lines

indicate radius of the secondary for different densities ranging from 1 to 7 g/cm³, this last density much larger than the expected values for minor bodies. The distance between the asteroid and the Sun is assumed again 1 AU. For lightness numbers higher than 8 the whole right branch of the g' family intersects the surface. The lightness number for a few representative asteroid missions are also indicated, showing that only for missions to very large asteroids such as Eros, where low lightness numbers are realistic, is this right branch feasible. The maximum ξ crossing of the g family decreases even more rapidly, falling below the asteroid surface already for values as low as 2. For relatively low lightness numbers, family g of “distant” prograde orbits or DPOs can thus no longer be considered distant.

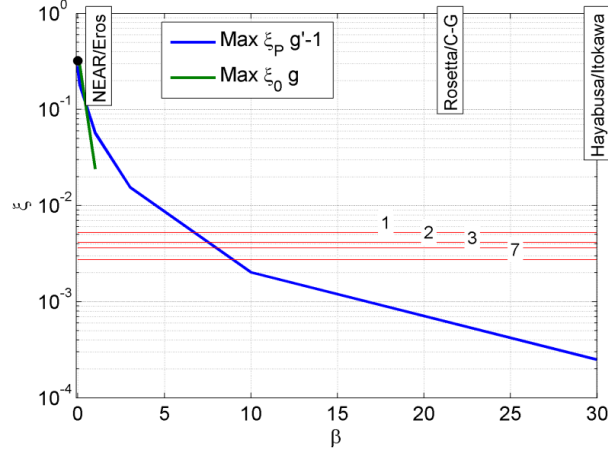


Figure 9: Maximum pericentre height of the simple-periodic g' branch and maximum ξ crossing of the g family. For large β_0 they fall below the body surface.

III. Stability of a and g' families of periodic orbits

Some of the orbit families have been shown to be unfeasible or non-existent for large lightness numbers. On the other hand, for the feasible branches and families, the stability of the periodic orbits needs to be taken into consideration to have usable and practical orbits for exploration. We concentrate on the family a and g' as they have feasible sections. From the results of Hénon,² in the Hill problem without SRP all a orbits and all g' double periodic are unstable, with two small sections of stable orbits in the simple-periodic branch.

A. Transition matrix propagation

In order to calculate the linear stability using Floquet theory, we obtain the state transition matrix Φ by integrating it together with the state vector along the trajectory for one orbital period.³² The extended equations of motion are given by:

$$\begin{bmatrix} \vec{\rho}' \\ \Phi' \end{bmatrix} = \begin{bmatrix} \vec{F}(\vec{\rho}) \\ \frac{\partial \vec{F}}{\partial \vec{\rho}} \Big|_{\vec{\rho}(\tau)} \end{bmatrix} \Phi \quad (12)$$

where $\vec{\rho}$ is the scaled state vector, \vec{F} the dynamics of the system presented in Eq. (9), and the initial conditions for the transition matrix integration is the identity matrix. The equations for the propagation of Φ in the photo-gravitational Hill problem are then given by:

$$[\Phi'] = \begin{bmatrix} [0] & [I] \\ \begin{bmatrix} 3 & 0 & 0 \\ 0 & 0 & 0 \\ 0 & 0 & -1 \end{bmatrix} - \frac{[I]}{|\vec{\rho}_{1-3}|^3} + 3 \frac{\vec{\rho}_{1-3} \cdot \vec{\rho}_{1-3}^T}{|\vec{\rho}_{1-3}|^5} & \begin{bmatrix} 0 & 2 & 0 \\ -2 & 0 & 0 \\ 0 & 0 & 0 \end{bmatrix} \end{bmatrix} [\Phi] \quad (13)$$

Once the state transition matrix is integrated over a full revolution, the monodromy matrix is calculated by mapping the transition matrix to the selected surface of section. The choice in initial conditions (a perpendicular crossing point of the ξ -axis with positive η') implicitly selects $\eta = 0$ as a surface of section. This results in a reduced state vector $\vec{\rho}^* = (\xi, \zeta, \xi', \zeta')^T$ in which the η and η' coordinates have been eliminated. Following Scheeres³² terminology, a series of auxiliary matrixes (P_0 , P_H and P_S) help map the transition matrix to the monodromy matrix. P_0 maps 1-to-1 the elements from the full state vector $\vec{\rho}$ that are maintained in our reduced state vector $\vec{\rho}^*$ (rows 2 and 5 are thus zero by our choice of surface of section and set of reduced state vector elements).

$$P_0 = \begin{bmatrix} 1 & 0 & 0 & 0 \\ 0 & 0 & 0 & 0 \\ 0 & 1 & 0 & 0 \\ 0 & 0 & 1 & 0 \\ 0 & 0 & 0 & 0 \\ 0 & 0 & 0 & 1 \end{bmatrix} \quad (14)$$

The following equation for P_H is here reproduced to report a typo in Eq. (6.19) from Ref. 32. It should state (more details on the nomenclature can be found in the cited reference):

$$P_H = -\hat{w}_{I+n} H_y \Big|_0 / H_{v_I} \Big|_0 \quad (15)$$

In our particular case, P_H is all zeros except for row 5, which contains the first order linear mapping of deviations in the reduced state vector to deviations in the eliminated coordinate η' . The relation between deviations in the reduced state vector coordinates and deviations on η' , assuming $d\Gamma = 0$ are given by:

$$\begin{aligned} \partial\eta' &= -\eta' + \sqrt{\eta'^2 + \partial\xi(6\xi + 2\beta_0 - 2/\xi^2) + \partial\xi^2(3 + 2/\xi^3)} \approx (3\xi + \beta_0 - 1/\xi^2) \partial\xi / \eta' \\ \partial\eta' &= -\eta' + \sqrt{\eta'^2 - \partial\xi'^2} \approx -\partial\xi'^2 / 2\eta' \\ \partial\eta' &= -\eta' + \sqrt{\eta'^2 - \partial\zeta'^2(1 - 1/\xi^3)} \approx -\partial\zeta'^2(1 - 1/\xi^3) / 2\eta' \\ \partial\eta' &= -\eta' + \sqrt{\eta'^2 - \partial\zeta'^2} \approx -\partial\zeta'^2 / 2\eta' \end{aligned} \quad (16)$$

There are only associated deviations of first order when considering the first coordinate, so only the first element of row 5 of matrix P_H is non-zero:

$$P_H(5,:) = \left[\frac{3\xi + \beta_0 - 1/\xi^2}{\eta'} \quad 0 \quad 0 \quad 0 \right]_{\tau=0} \quad (17)$$

The matrix $P_0 + P_H$ thus maps then initial deviations in the reduced state vector to initial deviations in the full state vector $\partial\vec{\rho}_0 = (P_0 + P_H)\partial\vec{\rho}_0^*$.

Finally P_S maps the final conditions after one period of propagation to the surface of section $\vec{\rho}|_{\eta=0} = P_S\vec{\rho}(\tau_f)$, taking into consideration the time derivatives of each component of the final position vector, and linearly mapping the matrix to $\eta = 0$.

$$P_S = I_{6 \times 6} - \vec{\rho}' [0 \quad 1 \quad 0 \quad 0 \quad 0 \quad 0] / \eta' \Big|_{\tau=\tau_f} \quad (18)$$

The monodromy matrix is obtained in the usual way as:

$$\Phi_M = P_0^T P_S \Phi(P_0 + P_H) \quad (19)$$

This results for our problem in a sparse 4x4 matrix, where the in-plane and out-of-plane dynamics appear to be decoupled. The monodromy matrix obtained can then be split into two 2x2 matrixes and the stability for each type of movement studied separately. The simplified condition for linear stability for each of them is then given by

$$\left| \text{Tr}(\Phi_{M,2 \times 2}) \right| < 2 \quad (\text{see Ref. 33})$$

B. Stability results and plots

With this stability criteria, family a remains always unstable, as was the case when solar radiation pressure was not introduced.

Figures 10 and 11 present the stability index (trace of the 2×2 monodromy matrix) for family g' as a function of the ξ crossing scaled with the ξ position of point L_2 . Orbits are stable for stability index between -2 and 2 . For the left branch of family g' , including the double-periodic section, orbits are mostly in-plane unstable for low lightness number, but become stable as the lightness number increases (see Figure 10 left), with the extreme case with large lightness numbers tending towards stability index equal to 2. Conversely, when considering out-of plane stability (see Figure 10 right), the family displays a somewhat opposite behaviour: the family presents regions of stability for low lightness numbers for certain ranges of ξ -axis crossings. However, it becomes unstable as the lightness number increases, and the extreme case tends again to a stability index equal to 2.

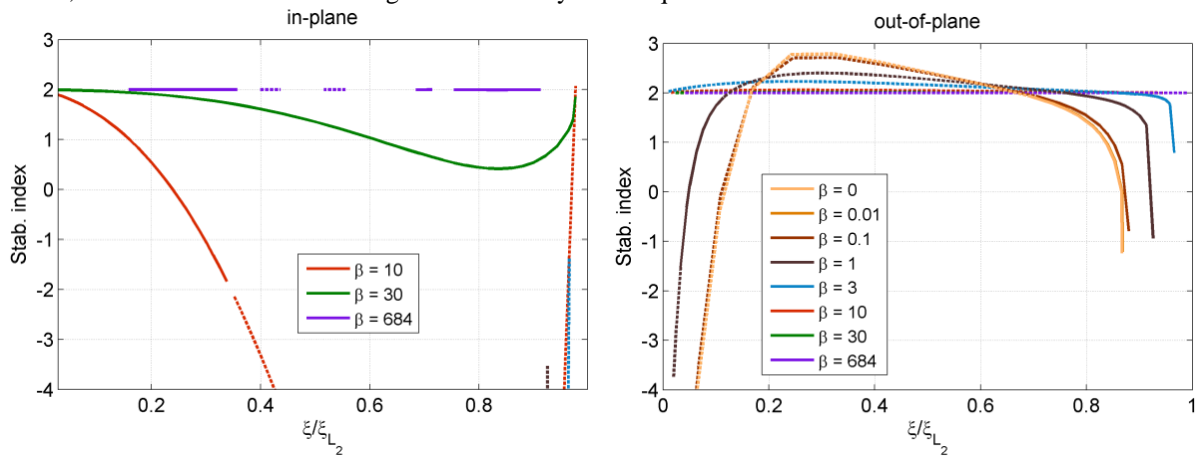


Figure 10: Stability of family g' left branch, in-plane (left) and out-of-plane (right)

On the other hand, the right branch of family g' , which is always simple-periodic, seems stable for most of the range when the lightness number is not zero, both in-plane and out-of plane (see Figure 11). However, this family consisted of orbits intersecting the surface of the secondary for large lightness numbers, questioning their applicability in the real world. Note also that the behaviour of this branch in the case of no SRP is intrinsically different for low ξ crossings, as it includes a different section of the $g-g'$ family.

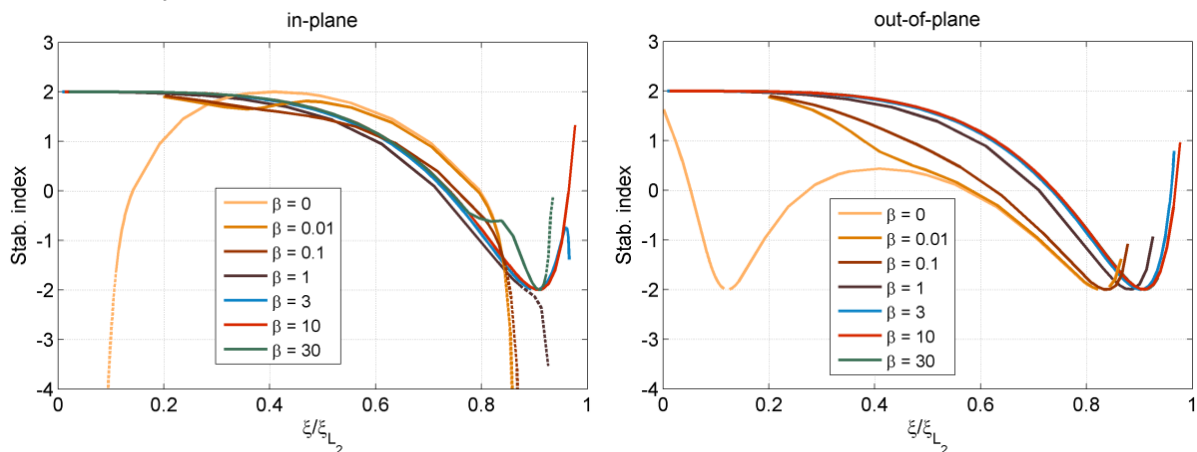


Figure 11: Stability of family g' right branch, in-plane (left) and out-of-plane (right)

IV. Further extensions

The analysis presented uses a simplified dynamics to study a particular set of periodic orbit families in the planar Hill problem with solar radiation pressure. Further exploration of periodic families and extended dynamic models are possible and desirable when applications for real asteroid missions are considered.

A. Additional families of periodic orbits

The analysis in this paper limits itself to the set of simple-periodic or double-periodic families studied by Hénon.² In the course of the study, various exotic and complex orbits were found belonging to the higher order periodicity families, still in the planar case (see Figure 12 for a sample of the trajectories found, mostly for low lightness numbers). Families up to multiplicity 81 were already reported in literature.²⁸ The family evolution, feasibility and stability analysis could be extended to N-periodic families. Despite the undeniable beauty of the wide range of solutions, their prospective usefulness is limited, due to frequent passes close to the asteroid, which could compromise the safety of a spacecraft when more perturbations are taken into consideration.

An additional possible extension is the study of three-dimensional periodic orbit families bifurcating from the planar ones or from known three-dimensional families such as halo orbits.

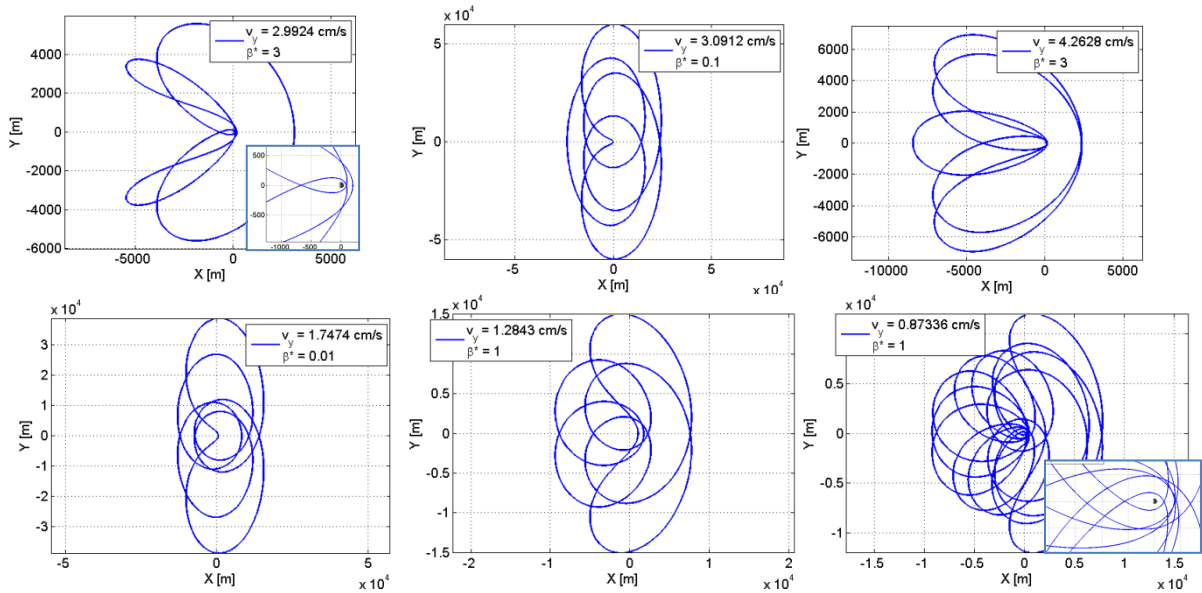


Figure 12: Additional families 3-periodic (1), 4-periodic (2, 3), 5-periodic (4, 5) and even 12-periodic (6)

B. Higher fidelity models

Regarding more complex dynamical models, a and g families can be reproduced with a full inertial numerical integration including SRP, eclipses, 3rd body perturbations and non-sphericity gravitational perturbations. The following equations of motion in an inertial frame incorporate the gravitational potential described as an expansion of spherical harmonics, and 3rd body perturbation of the Sun, again modified by a lightness number to represent SRP, but without the Hill's approximation:

$$\ddot{\vec{r}} = -\mu_A \frac{\vec{r}}{|\vec{r}|^3} - \mu_s \left(\frac{\vec{r}_{S-SC} (1 - \beta^*)}{|\vec{r}_{S-SC}|^3} - \frac{\vec{r}_{S-A}}{|\vec{r}_{S-A}|^3} \right) + \frac{\partial U_{NOSP}}{\partial r} \quad (20)$$

$$U_{NOSP}(r, \lambda, \theta) = \frac{\mu_A}{r} \sum_{n=2}^N (R/r)^n \sum_{m=0}^n P_{nm}(\sin \theta) (C_{nm} \cos m\lambda + S_{nm} \sin m\lambda)$$

Although the full numerical computation of the evolution and stability of symmetric periodic families is outside the scope of this paper, the effect of a few of these complications in the model is briefly discussed in this section.

1. Effect of eclipses

Eclipses have been modelled as an intersection of projected circles areas for the asteroid (assumed spherical) and the Sun,¹ which result in a modification in the lightness number value while on umbra or penumbra that depends of the intersection area ratio:

$$\beta^* = \beta \left(1 - \frac{A_{\cap}}{\pi R_{SUN}^2} \right) \quad (21)$$

Using Eq. (20) but excluding the gravitational harmonics potential, *a* and *g* families were calculated. The solution map for the *a* and *g*' double-periodic branch is plotted in Figure 13 for the extreme case of lightness number ~ 684 . Both families extend beyond the L_2 point, and the shape of the orbits dramatically changes for the cases spending a considerable time in eclipse (see Figure 14).

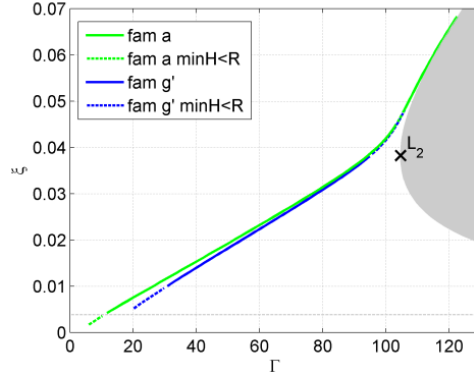


Figure 13: Solution map for the numerical propagation in the inertial frame with eclipses

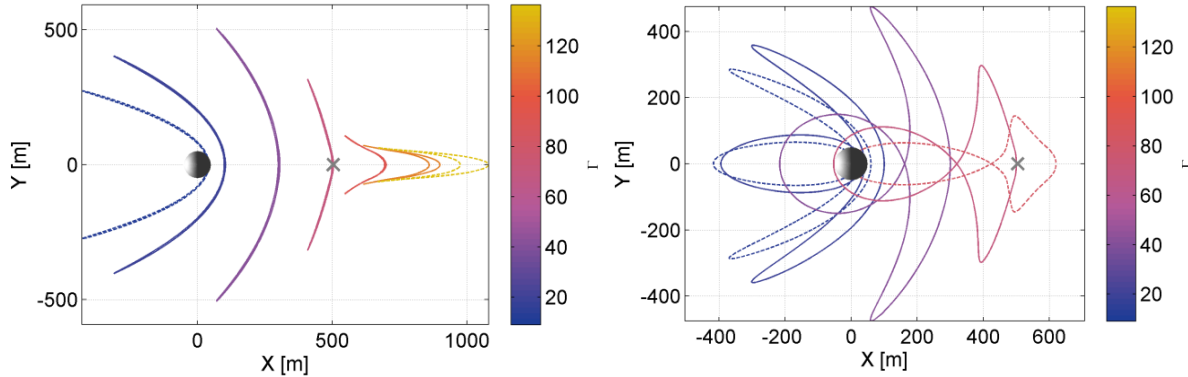


Figure 14: Families *a* and *g*' with numerical propagation in the inertial frame with eclipses. Extreme case of $\beta_0 \sim 684$

2. Non-sphericity perturbation

Higher order gravitational harmonics up to order 4 have been included in the propagation of orbits of the *g*' family, assuming a constant density tri-axial ellipsoid with axes $a = \sqrt{2}b = 2c$ rotating uniformly about an axis corresponding to its maximum moment of inertia. The rotational axis is assumed perpendicular to the orbital plane. It is interesting to observe that periodic orbits still exist with a more complex gravity model. However, the lightness number, or area to mass ratio required for a set of initial conditions in vertical velocity depends on the attitude of the asteroid at the initial time. A variable effective area controller might be required to maintain such an orbit when higher order gravitational harmonics are introduced, as was already suggested¹. Given the uncertainty in the mass, shape and associated gravity field of most asteroids, adjustable area or reflectivity would be a desired feature for orbiters that intend to benefit of SRP enabled exotic orbits. Figure 15 left plots the periodic orbit for a particular initial attitude of the asteroid and initial conditions, corresponding to 345 m x-coordinate. Figure 15 right shows the area required to maintain that particular orbit assuming a 100 kg spacecraft as a function of the initial angle γ_0 between the ellipsoid semimajor axis and the x-axis. The variations in area required are small and easily achievable by a variable reflectivity device such as the ones demonstrated on the Ikaros solar sail.³⁴

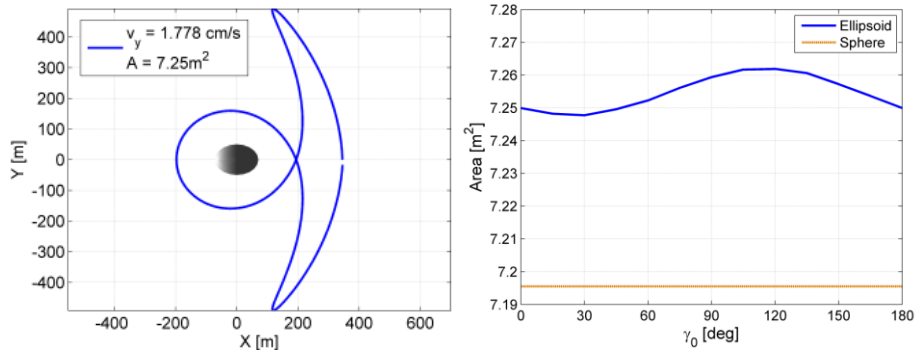


Figure 15: Double-periodic g class orbit example around a tri-axial ellipsoid (left), and area required for maintaining the periodic orbit as a function of initial ellipsoid orientation (right). Extreme case of $\beta_0 \sim 684$

C. Elliptical Restricted Three Body Problem

The analysis can also be extended to dynamical models of intermediate complexity, such as the Elliptical Restricted Three Body Problem (ER3BP), to account for a more representative case of an asteroid in an elliptical orbit around the Sun. Nonetheless, the characteristic time or period of the considered orbits is much smaller than the usual orbit periods of asteroids, so the variation in distance over a full revolution (which changes both the gravity attraction of the Sun and the SRP) would have a reduced effect in the shape and structure of these families. The existence of the g' family in the ER3BP has been demonstrated in literature.³⁵ There is no reason to doubt that these orbits could as well be extended to the case with non-zero lightness number.

V. Conclusions

The photogravitational Hill problem is a useful dynamical system to study the motion of spacecraft in the vicinity of asteroids. This paper has mapped the evolution of the a and $g-g'$ families of planar symmetric periodic orbits with the introduction of solar radiation pressure from the original Hill problem to an extreme case with very high lightness number. The structure of the solution space deviates from the original solution map in the original Hill problem, with the $g-g'$ family breaking apart into two unconnected families, one of which disappears for high lightness numbers.

The in-plane and out-of-plane stability of these sets of orbits has been calculated, and their feasibility in the case of a minor body has been analysed. Family a remains unstable as in the traditional Hill problem for all cases, while family $g-g'$ has certain regions of in-plane or out-of-plane stability. However, the most stable branch of this family becomes unfeasible for realistic asteroid densities and the high lightness numbers expected around small asteroids.

Acknowledgments

The work reported was supported by European Research Council grant 227571 (VISIONSPACE). The authors would also like to acknowledge the John Moyes Lessells Travel Scholarship of the Royal Society of Edinburgh, and the Mac Robertson Postgraduate Travel Scholarship for their support of the PhD placement at CU Boulder that led to the research presented in this paper. The attendance to the SPACE2014 conference to present this paper was kindly supported by the Royal Aeronautical Society Aerospace Speaker's Travel Grant.

References

- ¹ D. García Yárnoz, J.P. Sanchez Cuartielles, C.R. McInnes, Applications of Solar Radiation Pressure Dominated Highly Non-Keplerian Trajectories around Minor Bodies, in: 64th International Astronautical Congress, IAF, Beijing, China, 2013.
- ² M. Hénon, Numerical Exploration of the Restricted Problem. V. Hill's Case: Periodic Orbits and Their Stability, *Astronomy and Astrophysics*, 1, 1969, pp. 223-238.
- ³ T. Matukuma, On the Periodic Orbits in Hill's Case, *Proceedings of the Imperial Academy of Japan*, 6 (1), 1930, pp. 6-8.
- ⁴ T. Matukuma, Periodic Orbits in Hill's Case. Second Paper, *Proceedings of the Imperial Academy of Japan*, 8 (5), 1932, pp. 147-150.
- ⁵ T. Matukuma, Periodic Orbits in Hill's Case. Third Paper, *Proceedings of the Imperial Academy of Japan*, 9 (8), 1933, pp. 364-366.
- ⁶ G.H. Darwin, Periodic Orbits, *Acta Mathematica*, 21 (1), 1897, pp. 99-242.

- ⁷ R.A. Broucke, Periodic orbits in the restricted three-body problem with Earth-Moon masses, in: JPL technical report 32-1168, Jet Propulsion Laboratory, California Institute of Technology, Pasadena, 1968.
- ⁸ V. Szebehely, P. Nacozy, A Class of E. Strömngren's Direct Orbits in the Restricted Problem, *The Astronomical Journal*, 72 (2), 1967, pp. 184-190.
- ⁹ V. Szebehely, *Theory of orbits*, Academic Press, New York, New York, 1967.
- ¹⁰ M. Hénon, Exploration numérique du problème restreint. II. Masses égales, stabilité des orbites périodiques, *Annales d'Astrophysique*, 28, 1965, pp. 992-1007.
- ¹¹ E. Strömngren, Forms of periodic motion in the Restricted Problem and in the general Problem of Three Bodies, according to researches executed at the Observatory Copenhagen, *Publikationer og mindre Meddelelser fra Kobenhavns Observatorium*, 39, 1922, pp. 3-29.
- ¹² M. Hénon, Vertical Stability of Periodic Orbits in the Restricted Problem. I. Equal Masses, *Astronomy and Astrophysics*, 28, 1973, pp. 415-426.
- ¹³ M. Hénon, Vertical Stability of Periodic Orbits in the Restricted Problem. II. Hill's Case, *Astronomy and Astrophysics*, 30, 1973, pp. 317-321.
- ¹⁴ M. Michalodimitrakis, Hill's problem: families of three-dimensional periodic orbits, *Astrophysics and Space Science*, 68 (1), 1980, pp. 253-268.
- ¹⁵ L.M. Perko, Periodic solutions of the restricted problem that are analytic continuations of periodic solutions of Hill's problem for small $\mu > 0$, *Celestial mechanics*, 30 (2), 1982, pp. 115-132.
- ¹⁶ M. Hénon, New Families of periodic Orbits in Hill's Problem of Three Bodies, *Celestial Mechanics and Dynamical Astronomy*, 85 (223-246), 2003.
- ¹⁷ M. Hénon, Families of Asymmetric Periodic Orbits in Hill's Problem of Three Bodies, *Celestial Mechanics and Dynamical Astronomy*, 93 (1-4), 2005, pp. 87-100.
- ¹⁸ M. Lara, R. Russell, Concerning the family "g" of the restricted three-body problem, in: IX Jornadas de Trabajo en Mecanica Celeste, Jaca, Huesca, Spain, 2006.
- ¹⁹ M. Lara, R. Russell, B. Villac, Classification of the Distant Stability Regions at Europa, *Journal of Guidance, Control, and Dynamics*, 30 (2), 2007, pp. 409-418.
- ²⁰ A.B. Batkhin, Symmetric periodic solutions of the Hill's problem. I, *Cosmic Research*, 51 (4), 2013, pp. 275-288.
- ²¹ A.B. Batkhin, Symmetric periodic solutions of the Hill's problem. II, *Cosmic Research*, 51 (6), 2013, pp. 452-464.
- ²² P. Verrier, Connections between Halo families and prograde families in the Earth-Moon CRTBP, in: (unpublished), University of Strathclyde, 2013, pp. 1-11.
- ²³ Y.A. Chernikov, The Photogravitational Restricted Three-body Problem, *Soviet Astronomy - AJ*, 13 (1), 1970, pp. 176-181.
- ²⁴ J.F.L. Simmons, A.J.C. McDonald, J.C. Brown, The restricted 3-body problem with radiation pressure, *Celestial Mechanics*, 35, 1985, pp. 145-187.
- ²⁵ K.E. Papadakis, Families of Periodic Orbits in the Photogravitational Three-Body Problem, *Astrophysics and Space Science*, 245, 1996, pp. 1-13.
- ²⁶ V.V. Markellos, A.E. Roy, M.J. Velgakis, S.S. Kanavos, A Photogravitational Hill Problem and Radiation Effect on Hill Stability of Orbits, *Astrophysics and Space Science*, 271, 2000, pp. 293-301.
- ²⁷ S.S. Kanavos, V.V. Markellos, E.A. Perdios, C.N. Douskos, The Photogravitational Hill Problem: Numerical Exploration, *Earth, Moon and Planets*, 91, 2002, pp. 223-241.
- ²⁸ K.E. Papadakis, The Planar Photogravitational Hill Problem, *International Journal of Bifurcation and Chaos*, 16 (6), 2006, pp. 1809-1821.
- ²⁹ S.M. Byram, D.J. Scheeres, Spacecraft Dynamics in the Vicinity of a Comet in a Rotating Frame, in: AIAA/AAS Astrodynamics Specialist Conference, Honolulu, Hawaii, USA, 2008.
- ³⁰ S.B. Broschart, G. Lantoine, D.J. Grebow, Characteristics of Quasi-Terminator Orbits Near Primitive Bodies, in: 23rd Space Flight Mechanics Meeting, Lihue, Kauai, USA, 2013.
- ³¹ D.J. Scheeres, Solar Radiation Pressure: Exact Analysis, in: *Orbital Motion in Strongly Perturbed Environments: Applications to Asteroid, Comet and Planetary Satellite Orbiters*, Springer-Verlag Berlin Heidelberg, 2012, pp. 255-275.
- ³² D.J. Scheeres, Solution and Characterization Methods, in: *Orbital Motion in Strongly Perturbed Environments: Applications to Asteroid, Comet and Planetary Satellite Orbiters*, Springer-Verlag Berlin Heidelberg, 2012, pp. 143-169.
- ³³ D.J. Scheeres, Properties of Solution, in: *Orbital Motion in Strongly Perturbed Environments: Applications to Asteroid, Comet and Planetary Satellite Orbiters*, Springer-Verlag Berlin Heidelberg, 2012, pp. 105-141.
- ³⁴ R. Funase, O. Mori, Y. Tsuda, Y. Shirasawa, T. Saiki, Y. Mimasu, J. Kawaguchi, Attitude control of IKAROS solar sail spacecraft and its flight results, in: 61st International Astronautical Congress 2010, Prague, Czech Republic, 2010, pp. 4720-4725.
- ³⁵ S. Ichtiaroglou, Elliptic Hill's Problem: The Continuation of Periodic Orbits, *Astronomy and Astrophysics*, 92, 1980, pp. 139-141.